

Novel Magnetoacoustic Resonance Technique for Exploring Hidden Quadrupoles in a Crystal Field Quartet

Mikito Koga^{1*} and Masashige Matsumoto²

¹*Department of Physics, Faculty of Education, Shizuoka University, Shizuoka 422–8529, Japan*

²*Department of Physics, Faculty of Science, Shizuoka University, Shizuoka 422–8529, Japan*

Crystal field quartets with quadrupole degrees of freedom play a crucial role in hidden ordering systems, as exemplified by CeB₆. We present a novel magnetoacoustic resonance technique that combines acoustically induced strain fields with a linearly polarized high-frequency microwave field to probe quadrupoles inherent in the quartet hidden behind magnetic properties. This method offers the advantage of enabling quantum quadrupole resonance transitions for large excitation energy gaps within quartet sublevels under a strong magnetic field, which cannot be achieved by acoustic experiments alone. Formulating a simultaneous single-phonon–single-photon absorption transition process using Floquet theory, we demonstrate how the transition probabilities are affected by changing the propagation direction of a bulk acoustic wave. The key result is that distinct maxima in transition probabilities, attributed to specific propagation directions, indicate a characteristic of quadrupole physics and exhibit an abrupt change owing to an induced ordered moment. This photon-assisted magnetoacoustic resonance technique will promote a broader range of applications of acoustic experiments for the study of quadrupole physics.

1. Introduction

Crystal field multiplets, characterized by spin S (≥ 1), possess quadrupole degrees of freedom that can be coupled to strain fields induced by lattice deformations or to conjugate fields associated with local quadrupolar polarization.^{1,2} In various magnetic systems such as those involving f -electrons, the quadrupole properties, which are typically hidden behind the magnetic dipole responses, play a significant role in revealing rich phenomena not observed in purely dipolar magnetic systems.^{3,4} Theoretically, the quadrupoles at atomic sites are represented by rank-2 tensorial forms of local spin operators linked to charge distribution. It is crucial to elucidate how the crystal field multiplets exhibit such tensorial quadrupole characteristics, which remain difficult to access through conventional measurement techniques used in magnetic materials.

Cerium hexaboride (CeB₆) is an exemplary material for investigating the quadrupole physics associated with localized f -electrons.^{5,6} In the Ce $4f^1$ configuration, the sixfold degenerate f -electron state with total angular momentum $J = 5/2$ is stabilized by spin-orbit coupling and is split into Γ_8 quartet ground and Γ_7 doublet excited states within the O_h cubic crystal field environment.⁷ For the large Γ_8 – Γ_7 splitting (540 K in energy), one origin of a hidden order phase (phase II) appearing in CeB₆ at 3.4 K can be quadrupole degrees of freedom inherent in the Γ_8 quartet.⁸ The Γ_8 -based scenario for the emergence of an antiferroquadrupolar (AFQ) order was inferred in earlier experimental studies, including neutron scattering,⁹ nuclear magnetic resonance (NMR),¹⁰ and elastic constant measurements.¹¹ Notably, the B-site NMR line splitting was successfully explained by group theoretical studies considering an effect of a Γ_8 octupole induced by the AFQ ordered moment in the presence of a magnetic field.^{12–14} The field-induced octupole moment in the AFQ order phase was also confirmed by the results of resonant X-ray diffraction¹⁵ and inelastic neutron scattering experiments.¹⁶ Above the transition temperature, the robustness of the Γ_8 symmetry of the

Ce f^1 ground state was indicated by nonresonant inelastic X-ray scattering.¹⁷ Although Γ_8 quadrupoles are crucial for the emergence of the field-induced dipoles and octupoles, no direct conclusive evidence of the quadrupole dynamics has yet been obtained. Several issues concerning the local Γ_8 -based scenario have been raised by electron spin resonance (ESR) studies in high magnetic fields^{18–20} and by B-site nuclear quadrupole resonance in very low magnetic fields.²¹

In a different context, a spin-3/2 quartet can be realized as an electronic ground state of silicon vacancy (V_{Si}) centers in silicon carbide (4H-SiC), and this realization provides an intriguing platform operating four-level systems as qubits for quantum information technologies.^{22–28} Recent spin-acoustic experiments have revealed that the V_{Si} quartet can be coupled to strain fields induced by either a surface acoustic wave (SAW) propagating along the crystal surface or a bulk acoustic wave (BAW).^{29–31} The acoustically induced strain coupling is attributed to the quadrupole–strain (QS) interaction for spin-3/2 systems, and its quadrupole nature appears as an anisotropic spin-acoustic resonance under rotation of the static magnetic field.^{32,33} This observation motivated us to extend our previous study on magnetoacoustic resonance to uncover microscopic features of quadrupoles inherent in a crystal field quartet.³⁴ In the present study, in stead of rotating the magnetic field, we rotate the propagation direction of the acoustic wave so that the Zeeman splitting of the quartet is preserved. The profiles of quadrupoles can further be captured by measuring the propagation direction dependence of the acoustically driven quadrupole transition rates between quartet sublevels.

In conventional methods, there is a difficulty in applying the magnetoacoustic resonance to the case of large excitation energy gaps in a strong magnetic field (~ 1 T), which is inevitably required for precise measurements. Usually, an oscillating field of more than 10 GHz order is necessary for a resonance transition between two levels of a localized electron state. In contrast, the frequency of an acoustically

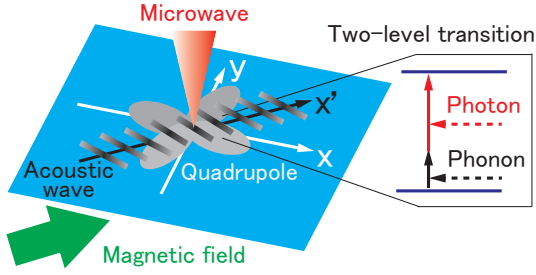


Fig. 1. (Color online) Illustration of photon-assisted magnetoacoustic resonance.³⁵⁾ The quadrupole resonance transition between two levels of a localized electron state is achieved through the simultaneous absorption of a single phonon and a single π -photon using an acoustic wave and a linearly localized microwave. The propagation direction (x' -axis) of the acoustic wave is rotated in the xy plane under a static magnetic field.

induced strain field is limited to the gigahertz order. In a recent study, we proposed photon-assisted magnetoacoustic resonance (PA-MAR) as an effective method for achieving quadrupole transitions involving such large excitations.³⁴⁾ In this method, a relatively low-frequency acoustically induced strain field is combined with a high-frequency linearly polarized microwave, as shown in Fig. 1.³⁵⁾ Importantly, absorption of the microwave photon (π -photon) drives only the longitudinal coupling with the two levels and does not affect the resonance transition. For an isolated electronic state, the resonance transition occurs owing to the simultaneous single-phonon–single-photon absorption, analogous to a two-photon absorption process with different frequencies, such as bichromatic driving for ESR using orthogonal electromagnetic waves.^{36–38)} In quadrupole–quadrupole interaction systems, ordered moments can be probed using the PA-MAR technique. At the quadrupolar ordering transition, slight mixing between the two levels may induce a transverse photon coupling, giving rise to an additional phonon–photon absorption process.

On the basis of the Floquet theory,³⁹⁾ we formulate the PA-MAR for the two-level system coupled to two periodically oscillating fields: a photon field and a phonon field with different frequencies.³⁴⁾ Although the longitudinal (diagonal) photon coupling does not contribute directly to the two-level transition, it plays an important role in effectively reducing the excitation energy. Consequently, the resonance transition becomes feasible despite the low frequency of the phonon field because of the transverse (off-diagonal) phonon coupling. Thus, the single-phonon absorption transition process can be potentially assisted by the single-photon absorption. We demonstrate how the PA-MAR transition probability depends on the propagation direction of the acoustic wave, focusing on the Γ_8 quartet for the typical magnetic field direction [110] in a cubic reference frame.

This paper is organized as follows. Section 2 presents the formulation of the PA-MAR for a two-level system using Floquet theory with a specific focus on the simultaneous single-phonon–single-photon absorption transition process. Section 3 discusses the time-averaged transition probability of PA-MAR for the low-lying states in the Γ_8 quartet coupled to inplane strain fields induced by a BAW. The BAW propagation direction is changed while the magnetic field is aligned along the [110] direction. We also clarify

how the induced AFQ ordered moment modifies the transition probability. Section 4 provides a summary of the main findings. Additional details are given in Appendices A, B, and C. Appendix A introduces a pseudospin-3/2 representation for the Γ_8 quartet considering the AFQ order in CeB₆. Appendix B discusses the case of a transverse BAW in comparison with that of a longitudinal BAW considered in Sect. 3.2. Appendix C offers a concise overview of the relationship between BAW propagation directions and displacement vectors within a cubic lattice.

2. Photon-assisted Magnetoacoustic Resonance

2.1 Two-level system coupled to photon and phonon fields

Let us begin with the two-level system coupled to periodically oscillating photon and phonon fields, as described by the following Hamiltonian:

$$H(t) = \frac{1}{2} \begin{pmatrix} -\varepsilon(t) & h^*(t) \\ h(t) & \varepsilon(t) \end{pmatrix}, \quad (1)$$

where

$$\varepsilon(t) = \varepsilon_0 + \Delta_L \cos(\omega_\Delta t + \theta) + A_L \cos \omega_A t, \quad (2)$$

$$h(t) = \Delta_T \cos(\omega_\Delta t + \theta) + A_T \cos \omega_A t. \quad (3)$$

The diagonal matrix elements are composed of the two-level splitting ε_0 , the longitudinal coupling to the photon field with amplitude Δ_L and frequency ω_Δ , and the longitudinal coupling to the phonon field with A_L and ω_A . Here, an initial phase shift θ is introduced to the photon field. For off-diagonal matrix elements, Δ_T and A_T represent the transverse coupling constants of the photon and phonon fields, respectively. The Schrödinger equation with the periodically time-dependent Hamiltonian,

$$i\hbar \frac{\partial \psi(t)}{\partial t} = H(t)\psi(t), \quad (4)$$

can be solved using Floquet theory, which is extended to the case of multifrequency. By substituting $\psi(t) = e^{-iqt}\phi(t)$ into this equation and applying the Fourier expansion³⁸⁾

$$H(t) = \sum_{nn'} H^{[n,n']} e^{i(n\omega_\Delta + n'\omega_A)t}, \quad \phi(t) = \sum_{nn'} \phi^{[n,n']} e^{i(n\omega_\Delta + n'\omega_A)t}, \quad (5)$$

we obtain the time-independent eigenvalue equation

$$\sum_{mm'} \{ H^{[n-m,n'-m']} + (n\omega_\Delta + n'\omega_A)\delta_{nm}\delta_{n'm'} \} \phi^{[m,m']} = q\phi^{[n,n]}, \quad (6)$$

and the solution is given for the quasi-energy q . Here, $\hbar = 1$ for brevity. This equation leads to the so-called Floquet Hamiltonian H_F ,

$$\langle \alpha nn' | H_F | \beta mm' \rangle = H_{\alpha\beta}^{[n-m,n'-m']} + (n\omega_\Delta + n'\omega_A)\delta_{\alpha\beta}\delta_{nm}\delta_{n'm'}, \quad (7)$$

and $H_{\alpha\beta}^{[n-m,n'-m']} \equiv \langle \alpha | H^{[n-m,n'-m']} | \beta \rangle$ for the two levels denoted by α and β . The infinite-dimensional matrix form of H_F is constructed on the basis of the Floquet states $|\alpha nn'\rangle = |\alpha\rangle \otimes |n\rangle \otimes |n'\rangle$ denoted by the indices of level α and integer n, n' ($= 0, \pm 1, \pm 2, \dots$) in Eq. (5). The practical calculation is performed by solving $H_F |q_\gamma\rangle = q_\gamma |q_\gamma\rangle$ with the γ th eigenvalue q_γ , and the corresponding eigenvector $|q_\gamma\rangle$ using the following

2×2 block matrices:

$$H^{(0,0]} = \frac{1}{2} \begin{pmatrix} -\varepsilon_0 & 0 \\ 0 & \varepsilon_0 \end{pmatrix}, \quad H^{[\pm 1,0]} = \frac{e^{\pm i\theta}}{4} \begin{pmatrix} -\Delta_L & \Delta_T^* \\ \Delta_T & \Delta_L \end{pmatrix},$$

$$H^{[0,\pm 1]} = \frac{1}{4} \begin{pmatrix} -A_L & A_T^* \\ A_T & A_L \end{pmatrix}. \quad (8)$$

For the other block matrices, $H^{[n-m,n'-m']} = \mathbf{0}$ (zero matrix) with $n-m = \pm 2, \pm 3, \dots$ ($n'-m' \neq 0$), and it holds for the replacement $(n, m) \leftrightarrow (n', m')$. To understand the structure of the matrix form of H_F , let us restrict the phonon sector to $n' = 0$ and $m' = -1$ for $A_L = 0$ and $\Delta_T = 0$. In the subspace of $\{|\alpha, n, 0\rangle, |\beta, m, -1\rangle\}$ ($n, m = \dots, -1, 0, 1, \dots$), the matrix form of H_F^{sub} is reduced to

$$H_F^{\text{sub}} = \begin{pmatrix} & & & \vdots & & \\ & \ddots & H^{[-1]} & \mathbf{0} & \mathbf{0} & \\ & & H^{[0]} & H^{[-1]} & \mathbf{0} & \dots \\ & & H^{[1]} & H_0^{[0]} & H^{[-1]} & \\ \dots & & \mathbf{0} & H_1^{[1]} & H_1^{[0]} & \\ & & \mathbf{0} & \mathbf{0} & H^{[1]} & \ddots \\ & & & \vdots & & \end{pmatrix}, \quad (9)$$

where

$$H_n^{[0]} = \begin{pmatrix} -(\varepsilon_0/2) - n\omega_\Delta & A_T^*/4 \\ A_T/4 & (\varepsilon_0/2) - \omega_A - n\omega_\Delta \end{pmatrix}, \quad (10)$$

$$H^{[\pm 1]} = \frac{e^{\pm i\theta}}{4} \begin{pmatrix} -\Delta_L & 0 \\ 0 & \Delta_L \end{pmatrix}. \quad (11)$$

A similar matrix of H_F^{sub} is obtained for the other phonon sectors $\{|\alpha, n, k'\rangle, |\beta, m, k' \pm 1\rangle\}$ (k' : integer) through the replacement $-(\varepsilon_0/2) \rightarrow -(\varepsilon_0/2) + k'\omega_A$ and $(\varepsilon_0/2) - \omega_A \rightarrow (\varepsilon_0/2) + (k' \pm 1)\omega_A$ in $H_n^{[0]}$. Alternatively, the above argument also holds in the subspace of the photon sectors $\{|\alpha, k, n'\rangle, |\beta, k \pm 1, m'\rangle\}$ (k : integer) for $A_T = 0$ and $\Delta_L = 0$, where the parameters are replaced as $\omega_\Delta \leftrightarrow \omega_A$ and $A_T \rightarrow \Delta_T e^{\pm i\theta}$ in $H_n^{[0]}$. In $H^{[\pm 1]}$, $\Delta_L \rightarrow A_L(\theta = 0)$.

2.2 Single-phonon–single-photon absorption transition

To describe the resonance transition driven by multifrequency fields, it is convenient to use the eigenstates of H_F for both $A_T = 0$ and $\Delta_T = 0$,⁴⁰⁾

$$|\alpha nn'\rangle_L = \sum_{k,k'=-\infty}^{\infty} e^{i(k-n)\theta} J_{k-n} \left(\frac{\Delta_L}{2\omega_\Delta} \right) J_{k'-n'} \left(\frac{A_L}{2\omega_A} \right) |\alpha kk'\rangle,$$

$$|\beta mm'\rangle_L = \sum_{k,k'=-\infty}^{\infty} e^{i(k-m)\theta} J_{k-m} \left(-\frac{\Delta_L}{2\omega_\Delta} \right) J_{k'-m'} \left(-\frac{A_L}{2\omega_A} \right) |\beta kk'\rangle, \quad (12)$$

with the k th Bessel function of the first kind J_k . The subscript L on the left-hand side indicates the longitudinal photon and phonon couplings. Here, we focus on the nearly degenerate Floquet states $|\alpha 00\rangle_L$ and $|\beta, -1, -1\rangle_L$ for the single π photon and single longitudinal phonon absorption processes under the condition $-\varepsilon_0/2 \simeq (\varepsilon_0/2) - \omega_\Delta - \omega_A$. When both A_T and Δ_T are finite, we treat these parameters as the perturbation,

$$\langle \alpha kk' | H_F' | \beta ll' \rangle = \frac{A_T^*}{4} \delta_{kl} (\delta_{k',l'+1} + \delta_{k',l'-1})$$

$$+ \frac{\Delta_T^*}{4} (e^{i\theta} \delta_{k,l+1} + e^{-i\theta} \delta_{k,l-1}) \delta_{k'l'}. \quad (13)$$

Using the formula for the Bessel function $J_n(a+b) = \sum_m J_m(a) J_{n-m}(b)$ and $J_{n-1}(a) + J_{n+1}(a) = (2n/a)J(a)$, we calculate the perturbation terms with A_T and those with Δ_T separately as

$$v_{k,k'}^A \equiv {}_L \langle \beta nn' | H_F' | \alpha mm' \rangle_L (\Delta_T = 0)$$

$$= \frac{A_T}{2} e^{ik\theta} J_k \left(\frac{\Delta_L}{\omega_\Delta} \right) \frac{k' \omega_A}{A_L} J_{k'} \left(\frac{A_L}{\omega_A} \right), \quad (14)$$

$$v_{k,k'}^\Delta \equiv {}_L \langle \beta nn' | H_F' | \alpha mm' \rangle_L (A_T = 0)$$

$$= \frac{\Delta_T}{2} e^{ik\theta} \frac{k \omega_\Delta}{\Delta_L} J_k \left(\frac{\Delta_L}{\omega_\Delta} \right) J_{k'} \left(\frac{A_L}{\omega_A} \right), \quad (15)$$

where $k = n - m$ and $k' = n' - m'$. In the subspace of the nearly degenerate Floquet states $|\alpha 00\rangle_L$ and $|\beta, -1, -1\rangle_L$, the 2×2 matrix form of the effective Hamiltonian,

$$H_{\text{eff}} = \begin{pmatrix} -\frac{\varepsilon_0}{2} + \delta & v_{-1,-1}^* \\ v_{-1,-1} & \frac{\varepsilon_0}{2} - \delta - \omega_A - \omega_\Delta \end{pmatrix}, \quad (16)$$

describes the transition at $\varepsilon_0 \simeq \omega_A + \omega_\Delta$. Here, the off-diagonal term $v_{-1,-1}$ is related to the peak broadening of the transition probability,

$$v_{-1,-1} = v_{-1,-1}^A + v_{-1,-1}^\Delta \simeq -\frac{e^{-i\theta}}{8} \left(\frac{A_T \Delta_L}{\omega_\Delta} + \frac{\Delta_T A_L}{\omega_A} \right), \quad (17)$$

for the weak coupling condition $|A_L|/\omega_A, |\Delta_L|/\omega_\Delta \ll 1$, where the approximation $J_k(a) = (-1)^k J_{-k}(a) \simeq (a/2)^k/k!$ ($k \geq 0$) is used. Like the Bloch–Siegert shift for the optically driven resonance transition, the energy shift δ is calculated using the second-order perturbation with respect to $v_{k,\pm 1}^A$ ($\propto A_T$) and $v_{\pm 1,k}^\Delta$ ($\propto \Delta_T$) as

$$\delta = - \sum_{\substack{k=-\infty \\ k \neq -1}}^{\infty} \left[\frac{|v_{k,-1}^A|^2}{\varepsilon_0 - \omega_A + k\omega_\Delta} + \frac{|v_{k,1}^A|^2}{\varepsilon_0 + \omega_A + k\omega_\Delta} \right. \\ \left. + \frac{|v_{-1,k}^\Delta|^2}{\varepsilon_0 - \omega_\Delta + k\omega_A} + \frac{|v_{1,k}^\Delta|^2}{\varepsilon_0 + \omega_\Delta + k\omega_A} \right]. \quad (18)$$

For weak coupling, the leading term of δ is represented by the sum of only the $k = 0$ terms,

$$\delta \simeq -\frac{\varepsilon_0 |A_T|^2}{8(\varepsilon_0^2 - \omega_A^2)} - \frac{\varepsilon_0 |\Delta_T|^2}{8(\varepsilon_0^2 - \omega_\Delta^2)}. \quad (19)$$

For the transition from $|\alpha\rangle$ to $|\beta\rangle$ in the two states, the time-averaged probability can be derived from the eigenvalues of H_{eff} as⁴⁰⁾

$$\bar{P}_{\alpha \rightarrow \beta} = \frac{1}{2} \frac{|v_{-1,-1}|^2}{|v_{-1,-1}|^2 + (\omega_\Delta + \omega_A - \varepsilon_0 + 2\delta)^2/4}. \quad (20)$$

In particular, we focus on $\bar{P}_{\alpha \rightarrow \beta}$ at $\varepsilon_0 = \omega_\Delta + \omega_A$ for the simultaneous single-phonon–single-photon absorption transition,

$$\bar{P}_{\alpha \rightarrow \beta}^{(1,1)} = \frac{1}{2} \frac{1}{1 + \gamma^2} \left(\gamma \equiv \frac{|\delta|}{|v_{-1,-1}|} \right), \quad (21)$$

except for $A_T = \Delta_T = 0$, and the ratio γ is obtained as

$$\gamma = \frac{|A_T|(1 + \bar{\omega}) \left(\frac{\bar{\omega}}{1 + 2\bar{\omega}} + \frac{1}{2 + \bar{\omega}} \frac{|\Delta_T|^2}{|A_T|^2} \right)}{|\Delta_L| \left| \bar{\omega} + \frac{\Delta_T A_L}{\Delta_L A_T} \right|} \left(\bar{\omega} \equiv \frac{\omega_A}{\omega_\Delta} \right) \quad (22)$$

$$\simeq \begin{cases} |A_T|/|\Delta_L| & (|\Delta_T|/|A_T| \ll \bar{\omega} \ll 1) \\ |\Delta_T|/(2|A_L|) & (\bar{\omega} \ll |\Delta_T|/|A_T| \sim |\Delta_L|/|A_L|). \end{cases}$$

3. Acoustically Driven Resonance Transition

3.1 Inplane quadrupole–strain interaction

For the quadrupole operators constructed by the spin $S = 3/2$ operators, we consider three components, namely,

$$O_u = \frac{1}{\sqrt{3}}(2S_z^2 - S_x^2 - S_y^2), \quad O_v = S_x^2 - S_y^2, \quad (23)$$

$$O_{xy} = S_x S_y + S_y S_x,$$

for the inplane (xy -plane) QS interaction. The lattice deformations in the xy -plane are described by the three components of the strain tensors $\varepsilon_{xx} = \partial u_x / \partial x$, $\varepsilon_{yy} = \partial u_y / \partial y$, and $\varepsilon_{xy} = [(\partial u_y / \partial x) + (\partial u_x / \partial y)]/2$, where $\mathbf{u} = (u_x, u_y, 0)$ is the displacement vector. The u - and v -type quadrupoles (O_u and O_v) are coupled to the corresponding strain tensors defined as $\varepsilon_u \equiv (2\varepsilon_{zz} - \varepsilon_{xx} - \varepsilon_{yy})/\sqrt{3}$ and $\varepsilon_v \equiv \varepsilon_{xx} - \varepsilon_{yy}$, respectively, and the xy type is coupled to ε_{xy} . The QS interaction Hamiltonian is given by^{41,42)}

$$H_\varepsilon = g_a O_u \varepsilon_u + g_b O_v \varepsilon_v + g_c O_{xy} \varepsilon_{xy}, \quad (24)$$

with the three independent coupling constants g_a , g_b , and g_c ($g_a = g_b$ is satisfied for O_h). For the magnetic field $\mathbf{H} \parallel \mathbf{Z} \parallel [110]$, we transform the quadrupole operators in Eq. (24) to those redefined in the (XYZ) reference frame using the unitary matrix U in Eq. (A.1). The unitary transformed O_k ($k = u, v, xy$) are given by the linear combinations of O_K ($K = U, V, YZ$),

$$U^\dagger O_u U = -\frac{1}{2} O_U + \frac{\sqrt{3}}{2} O_V, \quad U^\dagger O_v U = O_{YZ},$$

$$U^\dagger O_{xy} U = \frac{\sqrt{3}}{2} O_U + \frac{1}{2} O_V. \quad (25)$$

For the transformed QS interaction Hamiltonian,

$$\tilde{H}_\varepsilon = U^\dagger H_\varepsilon U = \sum_K A_K O_K, \quad (26)$$

the strain-dependent coupling coefficients are written as

$$A_U = -\frac{1}{2} g_a \varepsilon_u + \frac{\sqrt{3}}{2} g_c \varepsilon_{xy}, \quad A_V = \frac{\sqrt{3}}{2} g_a \varepsilon_u + \frac{1}{2} g_c \varepsilon_{xy},$$

$$A_{YZ} = g_b \varepsilon_v. \quad (27)$$

For the basis of $\{|3/2\rangle, |1/2\rangle, |-1/2\rangle, |-3/2\rangle\}$ with the quantization axis Z , the matrices of the corresponding quadrupole operators are given by³⁴⁾

$$\frac{O_U}{\sqrt{3}} = \begin{pmatrix} 1 & 0 & 0 & 0 \\ 0 & -1 & 0 & 0 \\ 0 & 0 & -1 & 0 \\ 0 & 0 & 0 & 1 \end{pmatrix}, \quad \frac{O_V}{\sqrt{3}} = \begin{pmatrix} 0 & 0 & 1 & 0 \\ 0 & 0 & 0 & 1 \\ 1 & 0 & 0 & 0 \\ 0 & 1 & 0 & 0 \end{pmatrix},$$

$$\frac{O_{YZ}}{\sqrt{3}} = \begin{pmatrix} 0 & -i & 0 & 0 \\ i & 0 & 0 & 0 \\ 0 & 0 & 0 & i \\ 0 & 0 & -i & 0 \end{pmatrix}, \quad (28)$$

respectively.

In the subsequent discussion, we concentrate on the two lowest-lying states of the crystal field quartet that participate in an antiferroquadrupolar ordering system exemplified by CeB₆, as described in Appendix A. The coupling coefficients with the phonon fields in Eqs. (2) and (3) are directly derived from the matrix elements of \tilde{H}_ε . In the subspace of $\{|\psi_{\mu,1}\rangle, |\psi_{\mu,2}\rangle\}$, which are the eigenstates of the mean field quadrupole–quadrupole interaction Hamiltonian $H_{\text{local}}^{(\pm)}$ for an induced quadrupole moment μ_{af} in Eq. (A.5), we obtain

$$A_L = \langle \psi_{\mu,2} | \tilde{H}_\varepsilon | \psi_{\mu,2} \rangle - \langle \psi_{\mu,1} | \tilde{H}_\varepsilon | \psi_{\mu,1} \rangle$$

$$= 2\sqrt{3}(-A_U \cos \theta_\lambda + A_V \sin \theta_\lambda) \cos 2\theta_\mu, \quad (29)$$

$$A_T = 2\langle \psi_{\mu,2} | \tilde{H}_\varepsilon | \psi_{\mu,1} \rangle = (\pm \tan 2\theta_\mu) A_L + i2\sqrt{3} A_{YZ}, \quad (30)$$

where $\cos \theta_\lambda = (16 + 3\lambda)/F_\lambda$ and $\sin \theta_\lambda = 15\sqrt{3}\lambda/F_\lambda$, using F_λ , as defined in Eq. (A.4). The parameter λ quantifies the anisotropy of the Zeeman effect for the Γ_8 quartet. In a similar way, the π photon field has the longitudinal coupling of $\Delta_L \propto \langle \psi_{\mu,2} | \tilde{J}_Z | \psi_{\mu,2} \rangle - \langle \psi_{\mu,1} | \tilde{J}_Z | \psi_{\mu,1} \rangle$, where these matrix elements are given in Eq. (A.7), and \tilde{J}_Z is the effective dipole operator described in Appendix A. The transverse photon coupling is generated by the induced quadrupole moment μ_{af} as $\Delta_T = (\pm \tan 2\theta_\mu) \Delta_L$. Rewriting $A_T \rightarrow |A_T| e^{i\theta_T}$, we obtain $\cos \theta_T = \pm \tan 2\theta_\mu (A_L/|A_T|)$. Because the finite moment μ_{af} also causes an additional energy splitting, γ in Eq. (21) is modified as $\gamma_\mu = |-\delta + (\delta\varepsilon_\mu/2)|/|v_{-1,-1}|$ for $|A_T|/\omega_\Delta, |\Delta_T|/\omega_A \ll 1$, where $\delta\varepsilon_\mu = (\omega_\Delta + \omega_A)[\sqrt{1 + (\bar{\mu}^2/E_0^2)} - 1]$ ($\bar{\mu}^2 \ll 1$). As defined in Eq. (A.6), E_0 is related to the Zeeman splitting ($\omega_\Delta + \omega_A = 2E_0 B$), and $\bar{\mu}$ represents the value of μ_{af} multiplied by D_Q/B . For the transition probability $\tilde{P}_{1 \rightarrow 2}^{(1,1)} = (1/2)(1 + \gamma_\mu^2)^{-1}$ between $|\psi_{\mu,1}\rangle$ and $|\psi_{\mu,2}\rangle$, γ_μ is calculated as

$$\gamma_\mu^2 = \frac{|A_T|^2}{\Delta_L^2} \frac{(1 + \bar{\omega})^2}{\bar{\omega}^2 + (1 + 2\bar{\omega}) \cos^2 \theta_T}$$

$$\times \left[\frac{\bar{\omega}}{1 + 2\bar{\omega}} + \frac{\tan^2 2\theta_\mu}{2 + \bar{\omega}} \frac{\Delta_L^2}{|A_T|^2} + \frac{4\omega_A \delta\varepsilon_\mu}{(1 + \bar{\omega})|A_T|^2} \right]^2, \quad (31)$$

where $\delta\varepsilon_\mu/\omega_\Delta \ll 1$ is assumed, and $\bar{\omega} \equiv \omega_A/\omega_\Delta$. The second term in the brackets $[\dots]$ is negligibly small compared with the last term for the weak coupling condition $|\Delta_L|/\omega_\Delta \ll 1$. As a result, Eq. (31) is simplified as

$$\gamma_\mu^2 = \frac{|A_T|^2}{\Delta_L^2} \frac{\bar{\omega}^2(1 + \bar{\omega})^2}{\bar{\omega}^2 + (1 + 2\bar{\omega}) \cos^2 \theta_T} \left(\frac{1}{1 + 2\bar{\omega}} + \frac{\bar{\mu}_{\text{eff}}^2}{1 + \bar{\omega}} \frac{\Delta_L^2}{|A_T|^2} \right)^2, \quad (32)$$

where the effective induced moment $\bar{\mu}_{\text{eff}}$ is defined as

$$\bar{\mu}_{\text{eff}}^2 \equiv 4(\omega_\Delta/\Delta_L)^2 (\delta\varepsilon_\mu/\omega_\Delta)$$

$$\simeq 2(1 + \bar{\omega})(\omega_\Delta/\Delta_L)^2 (\bar{\mu}/E_0)^2 \quad (\bar{\mu} \simeq 0). \quad (33)$$

Note that the calculated γ_μ is independent of the \pm signs of the staggered moment as defined in Eq. (A.5), i.e., $(\pm \tan 2\theta_\mu)$ in Eq. (30).

3.2 Quadrupole transition depending on propagation directions of a bulk acoustic wave

We consider that the local pseudo-quartet is coupled to the strain fields induced by a BAW propagating in the x' direction, denoted by angle φ , which is measured relative to the direction of the crystallographic x -axis. The x' and y' coordinates of BAW are transformed as

$$\begin{pmatrix} x' \\ y' \end{pmatrix} = \begin{pmatrix} \cos \varphi & \sin \varphi \\ -\sin \varphi & \cos \varphi \end{pmatrix} \begin{pmatrix} x \\ y \end{pmatrix}. \quad (34)$$

In this study, we focus on a longitudinal BAW considering the displacement of the vibration parallel to the propagation direction (x'). The three strain tensor components in Eq. (27) are replaced as

$$\varepsilon_{xx} \rightarrow -\frac{\varepsilon_{x'x'}}{\sqrt{3}}, \quad \varepsilon_{yy} \rightarrow \varepsilon_{x'x'} \cos 2\varphi, \quad \varepsilon_{xy} \rightarrow \frac{\varepsilon_{x'x'}}{2} \sin 2\varphi. \quad (35)$$

As indicated in Appendix C, the displacement vector \mathbf{u} is not parallel to the propagation direction in the xy plane of a cubic crystal, except for the principal [100] and diagonal [110] axes. As discussed subsequently, our focus is on the transition probabilities driven by the BAW propagating along the x' -axis in the vicinity of [110] ($\varphi = \pi/4$) and $[\bar{1}10]$ ($\varphi = 3\pi/4$). Consequently, we represent \mathbf{u} by the single component $u_{x'}$. Using Eq. (27), $|A_T|^2$ in Eq. (30) is given as a function of φ ,

$$|A_T|^2 = \left(\frac{\bar{\mu}}{F_\lambda E_{\bar{\mu}}} \right)^2 a_L(\varphi) + a_{YZ}(\varphi), \quad (36)$$

where

$$a_L(\varphi) = 4 [8(1 + 3\lambda)g_a + 3(4 - 3\lambda)g_c \sin 2\varphi]^2 \langle \varepsilon_{x'x'}^2 \rangle, \quad (37)$$

$$a_{YZ}(\varphi) = 12(g_b \cos 2\varphi)^2 \langle \varepsilon_{x'x'}^2 \rangle. \quad (38)$$

The square of the strain amplitude $\langle \varepsilon_{x'x'}^2 \rangle$ is represented by the average with respect to the spatial distribution of magnetic ions. In Eq. (36), $a_{YZ}(\varphi)$ approaches zero as $\varphi \rightarrow \pi/4$ ($x' \parallel H \parallel [110]$) and $\varphi \rightarrow 3\pi/4$ ($x' \perp H$). For these values of φ , we obtain $|A_T|^2/A_L^2 = (\bar{\mu}/E_0)^2$, and Eq. (32) is reduced to $\gamma_{\bar{\mu}}^2 = \bar{\mu}^2(2\omega_\Delta\omega_\Lambda)^2/(E_0\Delta_L A_L)^2$ under the condition $|\Delta_L|/\omega_\Delta \ll 1$. For other values of φ , the transition probability is not significantly affected by a finite $\bar{\mu}$.

In Fig. 2, we show the φ dependence of the transition probability for various values of $\bar{\mu}_{\text{eff}}^2$ ($= 10^4 \bar{\mu}^2$), considering the symmetric QS coupling case ($g_a = g_b = g_c \equiv g$). The other parameters are fixed as $\lambda = 4/9$, $\bar{\omega} = 0.1$, and $g^2 \langle \varepsilon_{x'x'}^2 \rangle / \Delta^2 = 1$. Here, the coupling strength Δ of the photon field is related to Δ_L as $\Delta_L = 2\Delta E_0^2 / E_{\bar{\mu}} = (2\Delta/3)(1 + 9\bar{\mu}^2)^{-1/2}$. As discussed above, the two peaks appear at $\varphi = \pi/4$ and $\varphi = 3\pi/4$, and their intensities show a marked reduction with the increase in $\bar{\mu}^2$. The difference between the φ dependence in $0 < \varphi < \pi/2$ and that in $\pi/2 < \varphi < \pi$ is due to the contribution from the term including $g_a g_c \sin 2\varphi$ in Eq. (37). At the peak for $\varphi = 3\pi/4$, the appearance of the dip signifies the competition between the QS coupling and quadrupole ordering effects. When the former effect is diminished by reducing the coupling g , a similar dip also emerges at $\varphi = \pi/4$ and deepens with the enhancement of $\bar{\mu}^2$.

This result demonstrates that the quadrupole components O_U and O_V in the longitudinal coupling are involved in the two-level transition when the O_{ZX} ordered moment $\bar{\mu}$ emerges. In the transverse coupling in Eq. (30), A_T contains

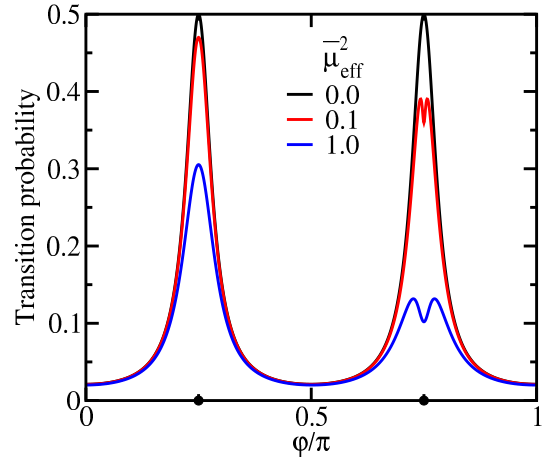


Fig. 2. (Color online) Transition probability $\bar{P}_{1 \rightarrow 2}^{(1,1)}$ plotted as a function of the BAW propagation direction φ for various values of the effective induced moment $\bar{\mu}_{\text{eff}}^2 = 0.0, 0.1, \text{ and } 1.0$. At the normal phase ($\bar{\mu}_{\text{eff}} = 0$), $\bar{P}_{1 \rightarrow 2}^{(1,1)}$ vanishes precisely at $\varphi/\pi = 1/4$ and $3/4$. Here, the magnetic field \mathbf{H} is parallel to the [110] direction ($\varphi = \pi/4$).

only A_{YZ} , and the single component O_{YZ} contributes to the transition in the normal phase. For a finite $\bar{\mu}$, the diagonal matrix element A_L (A_U and A_V) as well as A_{ZX} appears in A_T . Because of the two-level mixing, the abrupt change in transition probability is attributed to the quadrupole transition forbidden in the normal phase, which provides the evidence of the off-diagonal order such as O_{ZX} considered in the present study.

Finally, we mention that the single-photon absorption transition occurs for a finite $\bar{\mu}$ when ω_Δ is adjusted to the energy difference between $|\psi_{\mu,1}\rangle$ and $|\psi_{\mu,2}\rangle$. The photon-assisted single-phonon absorption transition can be observed as the sideband resonance.

4. Conclusion

We presented a theory of PA-MAR as a novel magnetoacoustic resonance technique, combining a π -photon field with acoustically induced strain fields to probe quadrupole characteristics of a crystal field quartet. Owing to an upper limit on acoustic wave frequencies, this method effectively realizes quadrupole resonance transitions for large excitation energy gaps under strong magnetic fields, which are inevitably required for precise measurements of the Γ_8 quartet quadrupoles in CeB_6 . On the basis of the Floquet theory, we developed a block matrix form of the Floquet Hamiltonian for a two-level system coupled to both periodically oscillating photon and phonon fields. In particular, we focused on the time-averaged PA-MAR transition probability under a weak coupling condition.

In this study, we investigated the quadrupole transition between the two lowest Γ_8 levels in a magnetic field along the [110] axis. The transition depends on a longitudinal BAW propagation direction φ measured from the [100] axis. The photon and phonon frequencies are fixed at the values tuned to satisfy the PA-MAR condition in the normal phase. The transition probability exhibits distinct peaks at $\varphi \rightarrow \pi/4$ ([110]) and $\varphi \rightarrow 3\pi/4$ ($[\bar{1}10]$), reflecting the fourfold symmetry of the quadrupole. These peaks show an abrupt reduction when an ordered moment is induced by the off-diagonal AFQ or-

der within the two levels. This behavior indicates that the quadrupole components contributing to the longitudinal coupling, which are inactive in the normal phase, participate in the PA-MAR transition process. Simultaneously, the transverse photon coupling is also generated.

Our proposal of PA-MAR is directly applicable to other pseudospin-3/2 quartets, such as the Re $5d^1$ electron state realized in the cubic Mott insulator $\text{Ba}_2\text{MgReO}_6$.^{43–45} In the $5d^1$ configuration, Γ_8 can be a ground state originating from the strong spin–orbit coupling for the threefold degenerate t_{2g} orbital. $\text{Ba}_2\text{MgReO}_6$ exhibits successive quadrupolar and magnetic ordering transitions at 33 K and 18 K, respectively. In the quadrupolar ordering phase, the coexistence of antiferroically arranged O_v and ferroically arranged O_u moments was observed. The origin of this exotic phenomenon has been attributed to the quadrupole components possessed by the Γ_8 quartet.⁴⁵ Therefore, it will be intriguing to confirm whether the experimentally observed quadrupole components are predominantly governed by Γ_8 and clarify the distinct quadrupole characteristics between the d -electron and f -electron systems. This distinction is nontrivial because crystal field effects generally dominate over spin–orbit coupling in localized d -electron states.⁴⁶

Acknowledgments The authors are deeply grateful to T. Yanagisawa for his insightful comments on the potential of optically assisted magnetoacoustic resonance measurements. This work was supported by JSPS KAKENHI Grant Number 21K03466.

Appendix A: Effect of Staggered Moment of Antiferroquadrupolar Order

We here consider the two lowest-lying states of the crystal field quartet involved in a quadrupolar order. One good example is the AFQ order in CeB_6 for the applied magnetic field $\mathbf{H} \parallel [110]$. The linear combination of the Γ_5 -type quadrupole components O_{yz} , O_{zx} , and O_{xy} ($O_{\mu\nu} = J_\mu J_\nu + J_\nu J_\mu$) is considered a prime candidate for the order parameter.^{12–16} Here, J_μ is a dipole component ($\mu = x, y, z$). The most dominant quadrupole coupling between the two states is associated with $O_{yz} + O_{zx}$ for $\mathbf{H} \parallel [110]$ in the cubic reference frame with the x , y , and z coordinates.^{12–14} When the Γ_8 quartet in the Ce f^1 configuration is represented by a pseudospin $S = 3/2$, the dipole and quadrupole operators are given by 4×4 matrices for the basis of the eigenstates of S_z , $\{|3/2\rangle, |1/2\rangle, |-1/2\rangle, |-3/2\rangle\}$. To calculate the quadrupole transition matrix elements, it is convenient to use a different reference frame where the in-plane field direction is chosen as the quantization axis Z , i.e., $\mathbf{H} = H\mathbf{e}_Z$ with $\mathbf{e}_Z = (1, 1, 0)/\sqrt{2}$. The other orthogonal unit vectors are defined as $\mathbf{e}_X = (0, 0, 1)$ and $\mathbf{e}_Y = (1, -1, 0)/\sqrt{2}$. For a finite magnetic field, it is convenient to transform the dipole and quadrupole operators defined in the cubic (xyz) reference frame to those redefined in the new (XYZ) reference frame using the unitary matrix,³⁴

$$U = \frac{1}{2\sqrt{2}} \begin{pmatrix} \chi^{-3} & \sqrt{3}\chi^{-3} & \sqrt{3}\chi^{-3} & \chi^{-3} \\ \sqrt{3}\chi^{-1} & \chi^{-1} & -\chi^{-1} & -\sqrt{3}\chi^{-1} \\ \sqrt{3}\chi & -\chi & -\chi & \sqrt{3}\chi \\ \chi^3 & -\sqrt{3}\chi^3 & \sqrt{3}\chi^3 & -\chi^3 \end{pmatrix}, \quad (\text{A.1})$$

where $\chi = e^{i\pi/8}$. This leads to $S_\mu = U^\dagger(\mathbf{e}_\mu \cdot \mathbf{S})U$ ($\mu = X, Y, Z$) for the dipole operator $\mathbf{S} = (S_x, S_y, S_z)$. The Zeeman splitting

for $\mathbf{H} \parallel Z$ is described by the Hamiltonian

$$H_Z = -g_J \mu_B H \sum_{i=1,2} E_{Z,i} |\psi_{Z,i}\rangle \langle \psi_{Z,i}|, \quad (\text{A.2})$$

for the two lowest-lying states:³⁴

$$|\psi_{Z,1}\rangle = c_+|3/2\rangle + c_-|-1/2\rangle, \quad |\psi_{Z,2}\rangle = -c_-|-3/2\rangle + c_+|1/2\rangle, \quad (\text{A.3})$$

where $|m\rangle$ ($m = \pm 1/2, \pm 3/2$) represents the eigenstates of S_Z , and

$$c_\pm = \pm \sqrt{\frac{1}{2} \left(1 \pm \frac{16 + 3\lambda}{F_\lambda} \right)}, \quad F_\lambda = \sqrt{(16 + 3\lambda)^2 + (15\sqrt{3}\lambda)^2}. \quad (\text{A.4})$$

In Eq. (A.2), μ_B is the Bohr magneton and g_J is Landé's g factor. For the eigenenergies, F_λ is related to $E_{Z,1} = (8 - 6\lambda + F_\lambda)/16$ and $E_{Z,2} = (-8 + 6\lambda + F_\lambda)/16$. Note that the Z component of the effective dipole operator in the two states is given by $\tilde{J}_Z = -\sum_{i=1,2} E_{Z,i} |\psi_{Z,i}\rangle \langle \psi_{Z,i}|$. The parameter λ represents an octupole effect that induces an anisotropic Zeeman effect. In the case of an f^1 Γ_8 quartet, λ is equal to $4/9$.

The quadrupole operator $O_{yz} + O_{zx}$ corresponds to O_{ZX} in the (XYZ) reference frame, and the latter generates an off-diagonal coupling between the two states as $\mu = |\psi_{Z,2}\rangle \langle \psi_{Z,1}| + |\psi_{Z,1}\rangle \langle \psi_{Z,2}|$. For the AFQ ordering, we define a staggered moment μ_{af} for the intersite O_{ZX} quadrupole–quadrupole interaction in the mean-field Hamiltonian for the localized electron states,³⁴

$$H_{\text{local}}^{(\pm)} = D_Q (\mp \mu_{\text{af}}) \mu + H_Z, \quad (\text{A.5})$$

where D_Q (> 0) represents the strength of the interaction, and the signs \pm of the first term are chosen for the two sublattice sites. The eigenvalue equation $H_{\text{local}}^{(\pm)} |\psi_{\mu,j}\rangle = B E_{\mu,j} |\psi_{\mu,j}\rangle$ ($B \equiv g_J \mu_B H$) is solved as $|\psi_{\mu,j}\rangle = \sum_{i=1,2} c_{ij} |\psi_{Z,i}\rangle$ with $E_{\mu,1} = -(F_\lambda/16) - E_{\bar{\mu}}$ and $E_{\mu,2} = -(F_\lambda/16) + E_{\bar{\mu}}$, where $E_{\bar{\mu}} = \sqrt{E_0^2 + \bar{\mu}^2}$, and

$$E_0 \equiv \frac{4 - 3\lambda}{8}, \quad \bar{\mu} \equiv \frac{D_Q \mu_{\text{af}}}{B}. \quad (\text{A.6})$$

The coefficients $\{c_{ij}\}$ are given by $c_{11} = c_{22} = \cos \theta_\mu$ and $c_{21} = -c_{12} = \pm \sin \theta_\mu$, which are related to $E_{\bar{\mu}}$ as $\cos 2\theta_\mu = E_0/E_{\bar{\mu}}$ and $\sin 2\theta_\mu = \bar{\mu}/E_{\bar{\mu}}$. Using these parameters, the induced quadrupole moment μ_{af} modifies the matrix elements of \tilde{J}_Z as

$$\begin{aligned} \langle \psi_{\mu,1} | \tilde{J}_Z | \psi_{\mu,1} \rangle &= -\frac{F_\lambda}{16} - E_0 \cos 2\theta_\mu, \\ \langle \psi_{\mu,2} | \tilde{J}_Z | \psi_{\mu,2} \rangle &= -\frac{F_\lambda}{16} + E_0 \cos 2\theta_\mu, \\ \langle \psi_{\mu,2} | \tilde{J}_Z | \psi_{\mu,1} \rangle &= \langle \psi_{\mu,1} | \tilde{J}_Z | \psi_{\mu,2} \rangle = E_0 (\pm \sin 2\theta_\mu). \end{aligned} \quad (\text{A.7})$$

Finally, we provide a brief comment on a correlation effect arising from intersite multipole–multipole interactions, including magnetic dipoles and octupoles other than the quadrupoles discussed above. This effect has not been considered in the mean-field treatment. For the AFQ ordering, the effect of an AF correlation between the two sublattice sites manifests as a modification of crystal field excitation, depending on the multipole–multipole coupling strength. Within the framework of our theory, an effective level shift of the excita-

tion energy can be incorporated into $\delta\varepsilon_\mu$ as a phenomenological parameter in Eq. (31). Consequently, the AF correlation effect may also contribute to the reduction in transition probability peak intensity discussed in Sect. 3.2.

Appendix B: Case of Transverse BAW

By analogy with the longitudinal BAW discussed in Sect. 3.2, we consider a transverse BAW vibrating in the xy -plane for $\mathbf{H} \parallel [110]$. The direction of displacement u_y is perpendicular to the BAW propagation direction (x'). The three strain tensor components are replaced as

$$\varepsilon_u \rightarrow 0, \quad \varepsilon_v \rightarrow -2\varepsilon_{x'y'} \sin 2\varphi, \quad \varepsilon_{xy} \rightarrow \varepsilon_{x'y'} \cos 2\varphi. \quad (\text{B.1})$$

For the transverse QS coupling, $|A_T|$ has the same form as Eq. (36), but it shows a different φ dependence:

$$a_L(\varphi) = [12(4 - 3\lambda)g_c \cos 2\varphi]^2 \langle \varepsilon_{x'y'}^2 \rangle, \quad (\text{B.2})$$

$$a_{YZ}(\varphi) = 48(g_b \sin 2\varphi)^2 \langle \varepsilon_{x'y'}^2 \rangle. \quad (\text{B.3})$$

As in Sect. 3.2, the same values are chosen for the parameters λ , $\bar{\omega}$, and $g^2 \langle \varepsilon_{x'y'}^2 \rangle / \Delta^2$. The PA-MAR transition probability $\bar{P}_{1 \rightarrow 2}^{(1,1)}$ shows sharp peaks when $\varphi \rightarrow 0, \pi/2$, and π in the normal phase ($\bar{\mu} = 0$), at which $a_{YZ}(\varphi)$ approaches zero. The induced ordered moment's increase in $\bar{\mu}$ causes an abrupt reduction in peak intensity, while preserving the fourfold symmetry with respect to φ . The fourfold symmetry is due to the vanishment of ε_u associated with the QS coupling (g_a) for the quadrupole component O_u , which is not generated by the transverse BAW. These characteristics of $\bar{P}_{1 \rightarrow 2}^{(1,1)}$ for the transverse BAW propagating along the principal crystallographic axes differ from those for the longitudinal BAW presented in Sect. 3.2. This distinction arises from the φ dependence of the transverse QS coupling (A_T).

Appendix C: Displacement Vector of BAW Propagating in Cubic Lattice

In general, the displacement vector \mathbf{u} of a propagating BAW is expressed as a linear combination of normal modes, each with its own distinct sound velocity. When the propagation direction is rotated in the cubic xy -plane, the eigenvector $\mathbf{u} = (u_x, u_y)$ of a normal mode is neither parallel nor orthogonal to the wave number vector $\mathbf{k} = (k_x, k_y) = k(\cos \varphi, \sin \varphi)$ for arbitrary values of φ except for $\varphi = 0, \pi/4, \pi/2, 3\pi/4$, and so on. This fact can be explained by solving the equations of motion for the BAW,⁴⁷⁾

$$\begin{cases} \rho \frac{\partial^2 u_x}{\partial t^2} = C_{11} \frac{\partial^2 u_x}{\partial x^2} + C_{44} \frac{\partial^2 u_x}{\partial y^2} + (C_{12} + C_{44}) \frac{\partial^2 u_y}{\partial x \partial y}, \\ \rho \frac{\partial^2 u_y}{\partial t^2} = C_{11} \frac{\partial^2 u_y}{\partial y^2} + C_{44} \frac{\partial^2 u_y}{\partial x^2} + (C_{12} + C_{44}) \frac{\partial^2 u_x}{\partial x \partial y}, \end{cases} \quad (\text{C.1})$$

using the mass density ρ and the bulk elastic constants C_{11} , C_{12} , and C_{44} for the cubic symmetry. For a traveling BAW with frequency ω , the components of the displacement vector are given as $u_j = u_{j,0} \exp[i(k_x x + k_y y - \omega t)]$ ($j = x, y$), where $u_{j,0}$ is the amplitude. Substituting u_j into Eq. (C.1), we obtain

$$\omega^2 \rho \begin{pmatrix} u_x \\ u_y \end{pmatrix} = \begin{pmatrix} C_{11}k_x^2 + C_{44}k_y^2 & (C_{12} + C_{44})k_x k_y \\ (C_{12} + C_{44})k_x k_y & C_{11}k_y^2 + C_{44}k_x^2 \end{pmatrix} \begin{pmatrix} u_x \\ u_y \end{pmatrix}, \quad (\text{C.2})$$

which leads to the condition for the solution $(u_x, u_y) \neq (0, 0)$:

$$\begin{aligned} & \left[\omega^2 \rho - \frac{k^2}{2}(C_+ + C_- \cos 2\varphi) \right] \left[\omega^2 \rho - \frac{k^2}{2}(C_+ - C_- \cos 2\varphi) \right] \\ & - \frac{k^4}{4} C_{2+}^2 \sin^2 2\varphi = 0. \end{aligned} \quad (\text{C.3})$$

Here, the elastic constants are rewritten as $C_\pm \equiv C_{11} \pm C_{44}$ and $C_{2+} \equiv C_{12} + C_{44}$. Introducing an effective elastic coefficient $C_\varphi \equiv (C_-^2 \cos^2 2\varphi + C_{2+}^2 \sin^2 2\varphi)^{1/2}$, we obtain the eigenvalues ω_\pm of frequency

$$\omega_\pm = \sqrt{\frac{C_+ \pm C_\varphi}{2\rho}} k. \quad (\text{C.4})$$

We concentrate on the eigenvector \mathbf{u} corresponding to ω_+ as a single normal mode. Using the relationship between C_- , C_{2+} , and C_φ with a new parameter φ_k ,

$$C_- \cos 2\varphi = C_\varphi \cos 2\varphi_k, \quad C_{2+} \sin 2\varphi = C_\varphi \sin 2\varphi_k, \quad (\text{C.5})$$

we obtain $u_x \sin \varphi_k = u_y \cos \varphi_k$ from Eq. (C.2). Since \mathbf{k} is parallel to the x' -axis, and $(u_{x'}, u_{y'})$ is related to (u_x, u_y) by the same transformation as given in Eq. (34), we obtain

$$u_{x'} \sin(\varphi_k - \varphi) = u_{y'} \cos(\varphi_k - \varphi). \quad (\text{C.6})$$

Combining Eqs. (C.5) and (C.6) and rewriting $\delta\varphi = \varphi_k - \varphi$, we derive

$$C_\varphi \begin{pmatrix} \cos 2\delta\varphi \\ \sin 2\delta\varphi \end{pmatrix} = \begin{pmatrix} \cos 2\varphi & \sin 2\varphi \\ -\sin 2\varphi & \cos 2\varphi \end{pmatrix} \begin{pmatrix} C_- \cos 2\varphi \\ C_{2+} \sin 2\varphi \end{pmatrix}. \quad (\text{C.7})$$

This leads to

$$\tan 2\delta\varphi = -\frac{\Delta C \sin 4\varphi}{1 + \Delta C \cos 4\varphi}, \quad (\text{C.8})$$

where

$$\Delta C \equiv \frac{C_{11} - C_{12} - 2C_{44}}{C_{11} + C_{12}}. \quad (\text{C.9})$$

An isotropic condition, $\Delta C = 0$, implies $\delta\varphi = 0$, indicating that $\mathbf{u} = (u_{x'}, 0)$ of a longitudinal BAW is parallel to the propagation direction (x') for arbitrary values of φ . Conversely, for $\Delta C \neq 0$, this holds at $\varphi = 0, \pi/4, \pi/2, 3\pi/4$, and so on. These values of φ correspond to $[100]$, $[110]$, $[010]$, and $[\bar{1}10]$, respectively. The analogous argument also applies to ω_- in Eq. (C.4), and $\mathbf{u} = (0, u_{y'})$ of a transverse BAW is orthogonal to the propagation direction (x').

*koga.mikito@shizuoka.ac.jp

- 1) S. Nakamura, T. Goto, S. Kunii, K. Iwashita, and A. Tamaki, J. Phys. Soc. Jpn. **63**, 623 (1994).
- 2) K. Mitsumoto, M. Akatsu, S. Baba, R. Takasu, Y. Nemoto, T. Goto, H. Yamada-Kaneta, Y. Furumura, H. Saito, K. Kashima, and Y. Saito, J. Phys. Soc. Jpn. **83**, 034702 (2014).
- 3) P. Santini, S. Carretta, G. Amoretti, R. Caciuffo, N. Magnani, and G. H. Lander, Rev. Mod. Phys. **81**, 807 (2009).
- 4) Y. Kuramoto, H. Kusunose, and A. Kiss, J. Phys. Soc. Jpn. **78**, 072001 (2009).
- 5) A. S. Cameron, G. Friemel, and D. S. Inosov, Rep. Prog. Phys. **79**, 066502 (2016).
- 6) See articles in *Rare-Earth Borides*, ed. D. S. Inosov (Taylor & Francis, New York, 2021).
- 7) K. R. Lea, M. J. M. Leask, and W. P. Wolf, J. Phys. Chem. Solids **23**,

- 1381 (1962).
- 8) F. J. Ohkawa, J. Phys. Soc. Jpn. **54**, 3909 (1985).
 - 9) J. M. Effantin, J. Rossat-Mignod, P. Burlet, H. Bartholin, S. Kunii, and T. Kasuya, J. Magn. Magn. Mater. **47&48**, 145 (1985).
 - 10) M. Takigawa, H. Yasuoka, T. Tanaka, and Y. Ishizawa, J. Phys. Soc. Jpn. **52**, 728 (1983).
 - 11) B. Lüthi, S. Blumenröder, B. Hillebrands, E. Zirngiebl, G. Güntherodt, and K. Winzer Z. Phys. B **58**, 31 (1984).
 - 12) R. Shiina, H. Shiba, and P. Thalmeier, J. Phys. Soc. Jpn. **66**, 1741 (1997).
 - 13) O. Sakai, R. Shiina, H. Shiba, and P. Thalmeier, J. Phys. Soc. Jpn. **66**, 3005 (1997).
 - 14) R. Shiina, O. Sakai, H. Shiba, and P. Thalmeier, J. Phys. Soc. Jpn. **67**, 941 (1998).
 - 15) T. Matsumura, T. Yonemura, K. Kunimori, M. Sera, F. Iga, T. Nagao, and J. Igarashi, Phys. Rev. B **85**, 174417 (2012).
 - 16) P. Y. Portnichenko, A. Akbari, S. E. Nikitin, A. S. Cameron, A. V. Dukhnenko, V. B. Filipov, N. Yu. Shitsevalova, P. Čermák, I. Radelytskiy, A. Schneidewind, J. Ollivier, A. Podlesnyak, Z. Huesges, J. Xu, A. Ivanov, Y. Sidis, S. Petit, J.-M. Mignot, P. Thalmeier, and D. S. Inosov, Phys. Rev. X **10**, 021010 (2020).
 - 17) M. Sundermann, K. Chen, H. Yavaş, H. Lee, Z. Fisk, M. W. Haverkori, L. H. Tjeng, and A. Severing, Europhys. Lett. **117**, 17003 (2017).
 - 18) A. V. Semeno, M. I. Gilmanov, A. V. Bogach, V. N. Krasnorussky, A. N. Samarin, N. A. Samarin, N. E. Sluchanko, N. Yu. Shitsevalova, V. B. Filipov, V. V. Glushkov, and S. V. Demishev, Sci. Rep. **6**, 39196 (2016).
 - 19) P. Schlottmann, Magnetochemistry **4**, 27 (2018).
 - 20) A. V. Semeno, S. Okubo, H. Ohta, and S. V. Demishev, Appl. Magn. Reson. **52**, 459 (2021).
 - 21) T. Mito, H. Mori, K. Miyamoto, T. Tanaka, Y. Nakai, K. Ueda, F. Iga, and H. Harima, J. Phys. Soc. Jpn. **92**, 034702 (2023).
 - 22) H. Kraus, V. A. Soltamov, D. Riedel, S. Váth, F. Fuchs, A. Sperlich, P. G. Baranov, V. Dyakonov, and G. V. Astakhov, Nat. Phys. **10**, 157 (2014).
 - 23) M. Widmann, S.-Y. Lee, T. Rendler, N. T. Son, H. Fedder, S. Paik, L.-P. Yang, N. Zhao, S. Yang, I. Booker, A. Denisenko, M. Jamali, S. A. Momenzadeh, I. Gerhardt, T. Ohshima, A. Gali, E. Janzén, and J. Wrachtrup, Nat. Mater. **14**, 164 (2015).
 - 24) D. Simin, H. Kraus, A. Sperlich, T. Ohshima, G.V. Astakhov, and V. Dyakonov, Phys. Rev. B **95**, 161201(R) (2017).
 - 25) R. Nagy, M. Widmann, M. Niethammer, D. B. R. Dasari, I. Gerhardt, Ö. O. Soykal, M. Radulaski, T. Ohshima, J. Vučković, N. T. Son, I. G. Ivanov, S. E. Economou, C. Bonato, S.-Y. Lee, and J. Wrachtrup, Phys. Rev. Appl. **9**, 034022 (2018).
 - 26) V. A. Soltamov, C. Kasper, A. V. Poshakinskiy, A. N. Anisimov, E. N. Mokhov, A. Sperlich, S. A. Tarasenko, P. G. Baranov, G. V. Astakhov, and V. Dyakonov, Nat. Commun. **10**, 1678 (2019).
 - 27) S. Castelletto and A. Boretti, J. Phys.: Photonics **2**, 022001 (2020).
 - 28) N. T. Son, C. P. Anderson, A. Bourassa, K. C. Miao, C. Babin, M. Widmann, M. Niethammer, J. U. Hassan, N. Morioka, I. G. Ivanov, F. Kaiser, J. Wrachtrup, and D. D. Awschalom, Appl. Phys. Lett. **116**, 190501 (2020).
 - 29) A. Hernández-Mínguez, A. V. Poshakinskiy, M. Hollenbach, P. V. Santos, and G. V. Astakhov, Sci. Adv. **7**, eabj5030 (2021).
 - 30) T. Vasselon, A. Hernández-Mínguez, M. Hollenbach, G. V. Astakhov, and P. V. Santos, Phys. Rev. Appl. **20**, 034017 (2023).
 - 31) J. R. Dietz, B. Jiang, A. M. Day, S. A. Bhave, and E. L. Hu, Nat. Electron. **6**, 739 (2023).
 - 32) A. Hernández-Mínguez, A. V. Poshakinskiy, M. Hollenbach, P. V. Santos, and G. V. Astakhov, Phys. Rev. Lett. **125**, 107702 (2020).
 - 33) M. Koga and M. Matsumoto, J. Phys. Soc. Jpn. **93**, 014703 (2024).
 - 34) M. Koga and M. Matsumoto, J. Phys. Soc. Jpn. **93**, 114701 (2024).
 - 35) T. Yanagisawa, JPSJ News and Comments **21**, 18 (2024).
 - 36) I. Gromov and A. Schweiger, J. Magn. Reson. **146**, 110 (2000).
 - 37) M. Kälin, I. Gromov, and A. Schweiger, Phys. Rev. A **69**, 033809 (2004).
 - 38) Z. György, A. Pályi, and G. Széchenyi, Phys. Rev. B **106**, 155412 (2022).
 - 39) J. H. Shirley, Phys. Rev. **138**, B979 (1965).
 - 40) S.-K. Son, S. Han, and S. I. Chu, Phys. Rev. A **79**, 032301 (2009).
 - 41) V. Dohm and P. Fulde, Z. Phys. B **21**, 369 (1975).
 - 42) B. Lüthi, *Physical Acoustics in the Solid State* (Springer, Heidelberg, 2005).
 - 43) C. A. Marjerrison, C. M. Thompson, G. Sala, D. D. Maharaj, E. Kermarrec, Y. Cai, A. M. Hallas, M. N. Wilson, T. J. S. Munsie, G. E. Granroth, R. Flacau, J. E. Greedan, B. D. Gaulin, and G. M. Luke, Inorg. Chem. **55**, 10701 (2016).
 - 44) D. Hirai and Z. Hiroi, J. Phys. Soc. Jpn. **88**, 064712 (2019).
 - 45) D. Hirai, H. Sagayama, S. Gao, H. Ohsumi, G. Chen, T. Arima, and Z. Hiroi, Phys. Rev. Res. **2**, 022063(R) (2020).
 - 46) H. Kubo, T. Ishitobi, and K. Hattori, Phys. Rev. B **107**, 235134 (2023).
 - 47) C. Kittel, *Introduction to Solid State Physics, 8th Edition* (John Wiley & Sons, Inc., New York, 2005).